Development 128, 631-643 (2001)
Printed in Great Britain © The Company of Biologists Limited 2001
DEV5434

Lineage, cell polarity and *inscuteable* function in the peripheral nervous system of the *Drosophila* embryo

Virginie Orgogozo, François Schweisguth* and Yohanns Bellaïche*

Ecole Normale Supérieure, UMR 8544 46, rue d'Ulm, 75230 Paris Cedex 05, France
*Authors for correspondence (e-mail: schweisg@wotan.ens.fr and bellaich@wotan.ens.fr)

Accepted 15 December 2000; published on WWW 7 February 2001

SUMMARY

The stereotyped pattern of the *Drosophila* embryonic peripheral nervous system (PNS) makes it an ideal system to use to identify mutations affecting cell polarity during asymmetric cell division. However, the characterisation of such mutations requires a detailed description of the polarity of the asymmetric divisions in the sensory organ lineages. We describe the pattern of cell divisions generating the vp1-vp4a mono-innervated external sense (es) organs. Each sensory organ precursor (SOP) cell follows a series of four asymmetric cell divisions that generate the four es organs cells (the socket, shaft, sheath cells and the es neurone) together with one multidendritic (md) neurone. This lineage is distinct from any of the previously proposed es lineages. Strikingly, the stereotyped pattern of cell divisions in this lineage is identical to those described for the embryonic chordotonal organ lineage and for the adult thoracic bristle lineage. Our analysis reveals that the vp2-vp4a SOP cells divide with a planar polarity to generate a dorsal pIIa cell and a ventral pIIb cell. The pIIb cell next divides with an apical-basal polarity to generate a basal daughter cell that differentiates as an md neurone. We found that Inscuteable specifically accumulated at the apical pole of the dividing pIIb cell and regulated the polarity of the pIIb division. This study establishes for the first time the function of Inscuteable in the PNS, and provides the basis for studying the mechanisms controlling planar and apical-basal cell polarities in the embryonic sensory organ lineages.

Key words: *Drosophila*, Sense organ, Lineage, Cell polarity, Inscuteable

INTRODUCTION

Most specialised functions of eukaryotic cells require subcellular asymmetries also referred to as cell polarity. During asymmetric cell division, cell polarity is revealed by the localisation of cell fate determinants at one pole of the mitotic spindle. The establishment of a polarity axis is therefore essential for the unequal segregation of cell fate determinants, and, hence, for the adoption of distinct identities by the two daughter cells. Studies in *Drosophila* have shown that at least two different signalling pathways can establish and maintain cell polarity during asymmetric cell division (Jan and Jan, 2000).

The first one depends on the activity of the *inscuteable* (*insc*) gene, which has been shown to regulate the asymmetric division of neuroblasts in the embryonic central nervous system (CNS). Following delamination from the neuroectoderm, neuroblasts divide with an apical-basal polarity to produce a neuroblast and a smaller ganglion mother cell (GMC). The *insc* gene is specifically expressed in neuroblasts as they delaminate (Kraut and Campos-Ortega, 1996; Kraut et al., 1996), and the Insc protein is recruited by Bazooka to the apical stalk of delaminating neuroblasts (Schober et al., 1999; Wodarz et al., 1999). A number of proteins, including Numb, Partner of Numb (Pon), Prospero (Pros) and Miranda localise to the basal pole and specifically segregate to the GMC (Hirata et al., 1995; Ikeshima-Kataoka et al., 1997; Knoblich et al., 1995; Lu et al., 1998; Rhyu et al., 1994; Shen et al., 1997; Spana and Doe, 1995). The activity of the *insc* gene is necessary to direct the basal localisation of Numb, Pon, Pros and Miranda during metaphase, and to orient the mitotic spindle perpendicularly to the plane of the epithelium (Kaltschmidt et al., 2000; Kraut et al., 1996; Yu et al., 2000). The polarising activity of the Insc protein depends on its direct binding to the Partner of Inscuteable (Pins) protein. Pins directly binds the Gαi protein, and possibly also the Gαo protein, suggesting that Insc might function by triggering a G protein signalling pathway (Parmentier et al., 2000; Schaefer et al., 2000; Yu et al., 2000).

A second signalling pathway depends on the activity of a seven-pass transmembrane receptor, Frizzled (Fz). During pupal development, Fz regulates the polarity of the bristle sensory organ precursor cell (SOP), also referred to as the primary precursor (pI) cell, which divides asymmetrically to produce the pIIa and pIIb cells (Gho and Schweisguth, 1998; Hartenstein and Posakony, 1989). This division is planar and oriented along the anterior-posterior (a-p) axis of the pupa. Numb and Pon localise to the anterior cortex of the pI cell and segregate to the anterior daughter cell, which will therefore adopt the pIIb fate (Gho and Schweisguth, 1998; Lu et al.,

1998; Rhyu et al., 1994; Uemura et al., 1989). Frizzled signalling orients the pI division along the a-p axis of the pupa and is also required for the strictly unequal segregation of the cell fate determinant Numb into only one of the pI daughter cell (Bellaïche et al., 2000; Gho and Schweisguth, 1998). The division of the pIIa cell is also planar and oriented along the a-p axis, while the pIIb cell is polarised perpendicularly to the plane of the epithelium (Gho et al., 1999). However, the orientation of the pIIa and pIIb divisions appear to be independent of *fz* (Gho and Schweisguth, 1998; R. Leborgne and F.S., unpublished observations), suggesting that additional mechanisms might control cell polarity in the peripheral nervous system (PNS).

A better understanding of the mechanisms regulating cell polarity during asymmetric division might benefit from an analysis of the numerous lethal mutations known to affect PNS development in the embryo (Jan et al., 1987; Kania et al., 1995; Salzberg et al., 1994). However, a phenotypic analysis of these mutations would first require the identification of the SOPs, their progeny cells and each division in these lineages. In the case of the embryonic mono-innervated external sense (es) organs, current models suggest that they are produced by two types of SOPs: the solo-es and the multidendritic (md)-es SOPs (Bodmer et al., 1989; Brewster and Bodmer, 1995; Vervoort et al., 1997). Results from both BrdU labelling and clonal analyses have indicated that the solo-es SOP generates, via a series of three asymmetric cell divisions, the four cells composing one es organ: the neurone, shaft, socket and sheath cells. The md-es SOP generates one additional cell, an md neurone. On the basis of clonal and mutant phenotypic analyses, two different models have been proposed for the md-es lineage (Brewster and Bodmer, 1995; Vervoort et al., 1997).

We describe the complete lineages produced by the five SOPs giving rise to the ventral papilla (vp) 1 to 4a (nomenclature according to Campos-Ortega and Hartenstein, 1997). Irrespectively of their previous classification as solo-es (vp1-4) or md-es (vp4a) SOPs, we found that these five SOPs, or pI cells, follow an identical series of four asymmetric divisions to generate one md neurone and the four cells forming one mono-innervated es organ. This md-es lineage differs from the two previously proposed md-es lineages in that the md neurone is generated by the division of the pIIb cell, identified here as the cell that has received Numb during the mitosis of pI. We also report that the division of the md-es pI cell is planar while the pIIb cell divides with an apical-basal polarity. Finally, the possibility of recognising each division allowed us to analyse the function of the *insc* gene in the embryonic PNS. We show that it directs the apical-basal polarity of the pIIb cell and regulates the specification of the md neurones in the embryo.

MATERIALS AND METHODS

Drosophila stocks

A yw stock was used as a wild-type stock. The AB44 line carries a PlacW enhancer-trap insertion at the *insc* locus (Kraut and Campos-Ortega, 1996). The E7-2-36 and A1-2-29 PlacW enhancer-trap lines express *lacZ* in md neurones, and in the socket and shaft cells, respectively (Bier et al., 1989). The CutA3 line carries a transgene expressing *lacZ* under the control of a *cut* enhancer (Jack and DeLotto, 1995). In this line, the cytoplasmic β-galactosidase protein specifically accumulates in the es cells from late stage 12 onwards. The $insc^{22}$ mutant allele behaves as a genetic null and carries a nonsense mutation at codon 82 (Buescher et al., 1998; Grzeschik et al., 1999). $insc^{22}$ homozygote embryos from $insc^{22}$/*Cyo,wg-lacZ* or $insc^{22}$, E7-2-36/*Cyo,wg-lacZ* stocks were identified by the absence of β-galactosidase staining.

Immunostaining and microscopy

Embryos were fixed and stained as previously described (The et al., 1999). Antibodies were used at the following dilutions: mouse anti-Cut, 1/1000 (DSBH); rat anti-Elav, 1/4 (DSBH); mouse anti-β-galactosidase, 1/5000 (Promega); rabbit anti-β-galactosidase 1/2000 (Cappel); rabbit anti-Pros, 1/1000 (gift of Y.-N. Jan); rabbit anti-Numb, 1/1000 (gift of Y.-N. Jan); rabbit anti-Miranda, 1/1000 (gift of F. Matsuzaki); and rabbit anti-Insc, 1/1000 (gift of B. Chia). Biotinylated, Alexa-488, Alexa-596, Cy5 anti-mouse, rat or rabbit, 1/1000 secondary antibodies were purchased from Molecular Probes or Jackson Laboratories. To detect Cut in the pI cell, the signal was amplified using the Renaissance kit (NEN). The DNA was stained using either TOTO-3 (1/3000, Molecular Probes) or propidium iodine (0,2 μg/ml, Sigma). Images were collected on a Leica NT confocal microscope and processed using NIH-image and Adobe Photoshop software. Figures show either a single confocal section or the maximal projection of several confocal *z* sections. In Figs 2C,D, 6C,C‴ and 9E, the CNS signal detected in the bottom *z* sections, i.e. below the vp1 organ, was reduced to better show the vp1 cells in the *z*-projected images.

RESULTS

The vp1-vp4a es organs are arranged in a circular arc in the ventral PNS

The external sensory organ cells are arranged in a segmental, highly stereotyped fashion, and each es organs cell can be reliably identified using anti-Cut antibodies in stage 16 embryos (Blochlinger et al., 1988; Blochlinger et al., 1990). In order to describe the pattern of cell divisions in the es organ lineage, we followed the divisions of the Cut-positive es precursor cells between stages 11 and 16. We focused our analysis on the five mono-innervated es organs located in the ventral region, vp1-vp4a, because this region is particularly outstretched following germ-band elongation, thus facilitating the identification of each es organ cell. In stage 16 embryos, the vp1-vp4a organs are arranged in a circular arc (Fig. 1). Each organ is composed of four Cut-positive cells. The socket and shaft cells, which lie within the epithelium, are strongly labelled by anti-Cut antibodies, whereas the neurone and the sheath cell, which are subepidermal, are more weakly labeled (Blochlinger et al., 1988; Blochlinger et al., 1990). The Elav and Pros proteins accumulate specifically in the neurone and in the shaft cell, respectively (Bier et al., 1988; Vaessin et al., 1991). The vp4a organ is found relatively close to the weakly Cut-positive anterior ventral md neurone called vdaa. A previous study has shown that the vdaa and vp4a cells are born from the same md-es lineage (Brewster and Bodmer, 1995). In the centre of the ventral region, the four vda_{A-D} and the ventral bipolar (vbp) md neurones, which are clustered together, are also weakly labeled by anti-Cut antibodies.

pI divides within the plane of the epithelium and along the dorsal-ventral axis

At stage 11, five isolated cells that accumulate Cut appear at

stereotyped positions in the ventral region. Based on their position, these cells correspond to the pI cells of the five vp1-vp4a organs. We took advantage of the slight asynchrony observed in the timing of the pI divisions from one segment to another to establish the origin of the increasing number of Cut-positive cells. Indeed, we noticed that cell divisions in the vp1-vp4a lineages tend to occur slightly earlier in anterior segments relative to more posterior ones (Fig. 2A,A′). The observation of a single Cut-positive pI cell dividing at the vp2 position in the abdominal hemisegment A7 and of two Cut-positive cells at the same position in A6 led us to conclude that the two cells observed in A6 are sister cells born from one pI cell (Fig. 2A,A′). Thus, lineage relationship could be inferred from the direct observation of dividing cells on fixed samples.

The analysis of the positions of the two pI daughter nuclei at telophase indicates that pI divides within the plane of the epithelium (Fig. 3B). Numb localises asymmetrically in pI at metaphase and is inherited by one of the two daughter cells at telophase (Fig. 3A,B). The pI daughter cell inheriting Numb is the pIIb cell and its sister is pIIa. In the case of the vp2-vp4a organs, the two daughter nuclei are positioned along the dorsal-ventral (d-v) axis, and Numb forms a ventral crescent at metaphase and segregates to the ventral daughter cell at telophase (Fig. 3D). We conclude that, at the vp2-vp4a position, pI divides with a stereotyped d-v planar polarity. In contrast, the division of the vp1 pI cell is randomly oriented within the plane of the epithelium with Numb segregating in only one daughter cell (Fig. 3D).

pIIb divides asymmetrically with an apical-basal polarity

At stage 12, the anterior-ventral cell of each pIIa-pIIb cell pair seen at the vp2-vp4a position enters mitosis (Figs 2B, 3E). The position of the daughter nuclei relative to the surface of the embryo at telophase indicates that pIIb divides roughly perpendicular to the plane of the epithelium (Fig. 4B). The orientation of the pIIb division was confirmed by analysing the orientation of the mitotic spindle and the position of the centrosomes (data not shown), but we could not measure precisely the orientation of the mitotic spindle in the dividing pIIb cell because the curvature of the epithelium in the gastrulating embryo precludes a precise determination of its orientation relative to the epithelial surface. Numb, Pon, Miranda and Pros, which is first detected in the dividing pIIb cell, localise to the basal pole of the pIIb cell at metaphase (Fig. 4A,C,C′ and data not shown) and segregate to the basal daughter cell (Fig. 4B,D,D′). Noticeably, at telophase, the basal daughter cell appears to be significantly smaller than its apical sister (Fig. 4B). This indicates that pIIb generates two cells of different size. However, following pIIb division, no difference in nuclear size is detected using the Pros and Cut markers. We conclude that, at the vp2-vp4a position, the pIIb division is polarised along the apical-basal axis of the epithelium.

At the vp1 position, one of the two pI daughter cells expresses Pros and divides with an apical-basal polarity to generate a basal cell that inherits both Numb and Pros (data not shown). Based on these observations, we conclude that the second cell division observed at the vp1 position is the pIIb division, as shown for the vp2-vp4a positions.

We called X the small basal pIIb daughter cell that has specifically inherited Pros, and pIIIb its apical sister. Soon after the pIIb division, the only es cell to accumulate Pros is the X cell (Fig. 4D,D′; see also vp2 in Fig. 2B,B′). In early stage 13 embryos, in which all pIIb cells have divided, two Pros-positive cells are observed: the basal highly Pros-positive X cell and the apical weakly Pros-positive pIIIb cell (Fig. 4E,E′; see also the legend to Fig. 7).

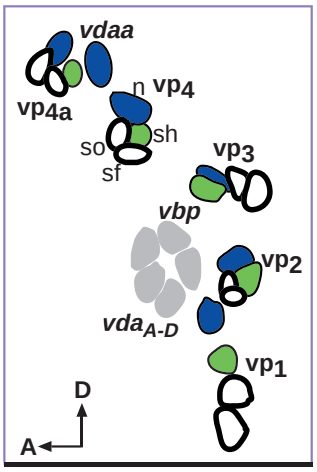

Fig. 1. The vp1-vp4a es organs form a circular arc at stage 16. Diagram of the vp1-vp4a mono-innervated es organ cells and the vdaa, $vda_{A\text{-}D}$ and vbp md neurones in the ventral region of the A1-7 hemisegments. (Nomenclature according to Campos-Ortega and Hartenstein, 1997.) The socket (so) and shaft cells (sf), which accumulate a high level of Cut, are shown in white. The Cut- and Pros-positive es sheath cells (sh) are in green and the Cut- and Elav-positive es neurones (n) are in blue. The vdaa md neurone, which has been shown to be related by lineage to the vp4a organ, is in blue (Brewster and Bodmer, 1995). The $vda_{A\text{-}D}$ and vbp neurones are in grey.

pIIa divides next to generate the socket and shaft cells and pIIIb divides last

At early stage 13, a Pros-negative pIIa cell entering mitosis can be observed (Fig. 5A,A′; see also vp2 from segment A3 in Fig. 2C,C′), while clusters of four cells are seen at the corresponding position in adjacent hemisegments. These clusters contain the highly Pros-positive X cell, the weakly Pros-positive pIIIb cell and two Pros-negative cells (Fig. 5B,B′; see also vp2 from segment A5 in Fig. 2C,C′). We conclude that the two Pros-negative cells are the pIIa daughter cells. These cells are localised in the superficial epidermal layer and are strongly Cut positive (Figs 5B, 2C). These two strongly Cut-positive cells are observed in the epidermis at the vp1-vp4a positions from stage 13 onwards (Fig. 2D). At stage 16, these two cells express A1-2-29, a socket and shaft cell marker (data not shown). These observations indicate that the division of pIIa generates the socket and shaft cells.

At late stage 13, the weakly Pros-positive pIIIb cell enters mitosis (Fig. 5C). Pros is asymmetrically localised in dividing pIIIb and is inherited by only one daughter cell at telophase (Fig. 5C-D″). We also observed that the X and pIIIb cells both accumulate Elav, a neuronal marker. The X cell can be easily identified as it accumulates a higher level of Elav. In contrast to Pros, Elav segregates equally into the two pIIIb daughter cells at telophase (Fig. 5D-D″). Following the pIIIb division,

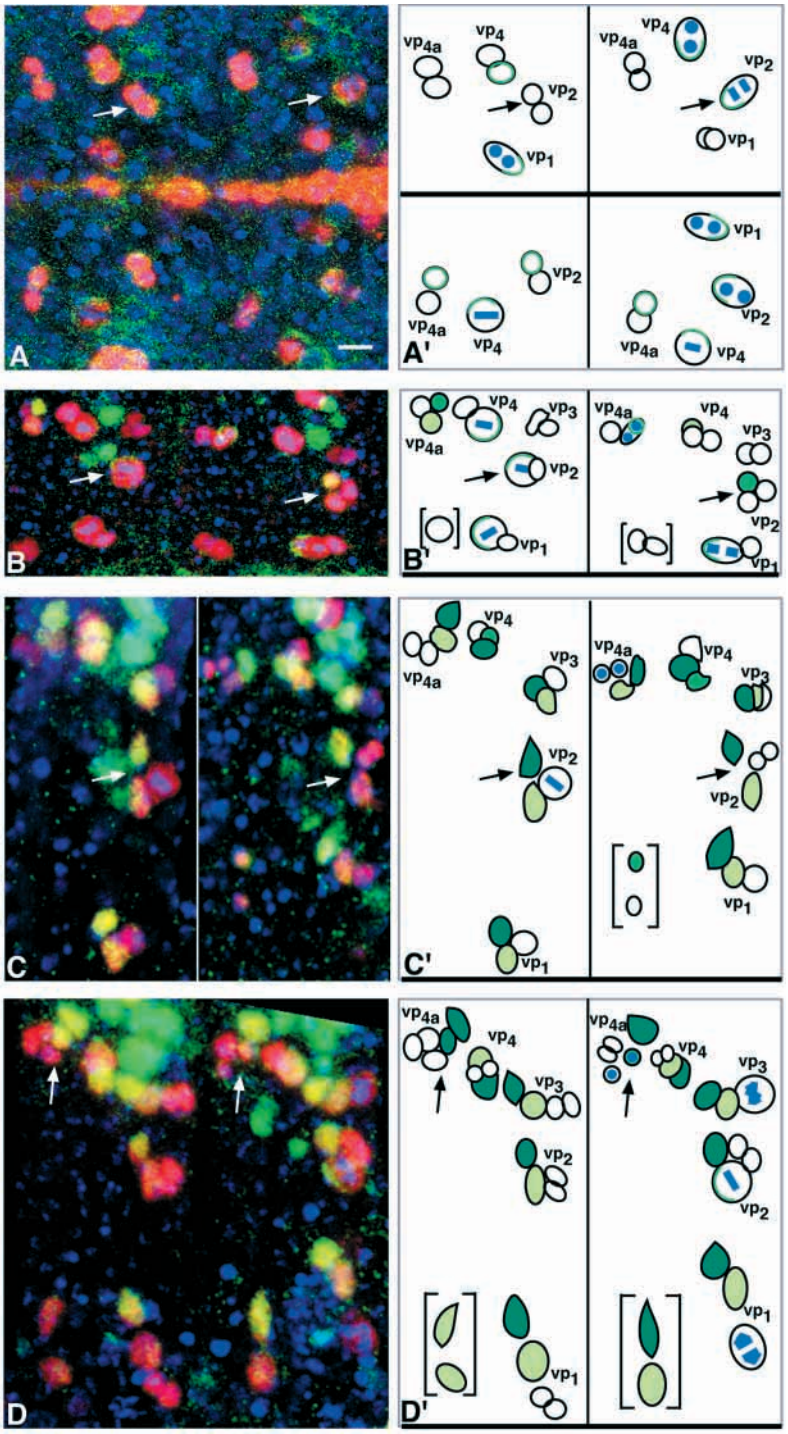

Fig. 2. Establishing the pattern of cell divisions in the vp1-vp4a lineages. (A-D) Embryos stained for Cut (red), DNA (blue) and Numb (green in A) or Pros (green in B,C,D) are shown on the left. (A′-D′) Corresponding schematic representations of the Cut-positive cells are presented on the right. In this representation, mitotic DNA is in blue, and Numb (A′) or Pros (B′,C′,D′) is in green. Dividing cells were identified based on DNA staining and on the diffuse Cut staining, which reveals nuclear envelope breakdown. Because several confocal sections were projected to visualise all PNS Cut-positive cells, some Cut-positive cells do not appear as individually labelled nuclei (see vp1 in A′ for example). Importantly, all *z* sections were analysed to draw the diagrams shown in A′, B′, C′ and D′. The ventral midline and the intersegmental borders are represented by horizontal and vertical black lines, respectively. (A,A′) Ventral view of the segments A6 (left) and A7 (right) in a stage 11 embryo. The vp1-vp4a precursor cells are found at symmetrical positions on either side of the ventral midline, which is also Cut positive, thus facilitating their identification. In this embryo, the vp3 pI cells and some vp1 pI cells cannot yet be detected using Cut as a marker. Based on Cut immunoreactivity, the pI cells appear in the following order: vp4a > vp2 > vp4 > vp1 > vp3. In segment A7, the vp2 pI cell is in anaphase (arrow), with Numb segregating to the ventral daughter cell, while two Cut-positive cells are seen at the vp2 position in segment A6 (arrow). This illustrates how a lineage relationship can be established between a dividing precursor cell and its two daughter cells by comparing identical positions in adjacent segments. (B,B′) Lateral view of the segments A1 (left) and A2 (right) in a stage 12 embryo. At the vp2 position in A1 (left arrow), the pIIb cell is in metaphase. At the vp2 position in A2 (right arrow), three cells are seen, including one basal Pros-positive cell (in green). At the vp4a position in A1, three cells are detected, one highly Pros-positive cell (dark green), one weakly Pros-positive cell (light green) and one Pros-negative cell. At this stage, one or two clustered Cut-positive cells are also observed anteriorly to the vp1 position (square brackets in B′). (C,C′) Lateral view of the segments A3 (left) and A5 (right) of an early stage 13 embryo. At the vp2 position in A3 (left arrow), the Pros-negative cell is in metaphase. In A5, at the same position (right arrow), two Pros-negative and highly Cut-positive cells are observed next to the two Pros-positive cells. In addition to the vp1-vp4a cells, one Cut-positive cell is found anteriorly to the vp1 position in A5 (square brackets in C′). This cell is in telophase and Pros is asymmetrically partitioned into the dorsal daughter cell. The precise relationship between this mitotic cell and the Cut-positive cells observed at this position in stage 12 embryos (B,B′) was not established. (D,D′) Lateral view of the segments A2 (left) and A3 (right) of a late stage 13 embryo. At the vp4a position in A3 (right arrow), one of four vp4a cell is in telophase, with Pros segregating unequally into the dorsal daughter cell. At the vp4a position in A2, five cells are seen. Anteriorly to the vp1 cell, two Cut-positive cells can be seen (square brackets in D′) with the dorsal-most cell accumulating a higher level of Pros. These two cells may be born from the mitotic cell observed at this position in stage 12 embryos (square brackets in C′). Scale bar: 5 μm.

the vp1-vp4a clusters are composed of five cells: the socket and shaft cells, the two pIIIb daughter cells and the X cell.

The X cell adopts an md fate

At stage 13, each X cell occupies a stereotyped position. The vp4a X cell is located dorsally between the vp4a and vp4 clusters, and each of the vp1-vp4 X cells is found nearest the centre of the circular arc formed by the vp1-vp4a cells (Fig. 6A-B″; see also Fig. 2C,D). The accumulation of Elav in the X cell indicates that X may become a neurone. To determine the fate of the X cell, we have compared the position of the Pros- and Elav-positive X cells in adjacent hemisegments of late stage 13 embryos (Fig. 6A-B″). This analysis suggests that the vp1-vp4 X cells migrate towards the centre of the vp1-vp4a

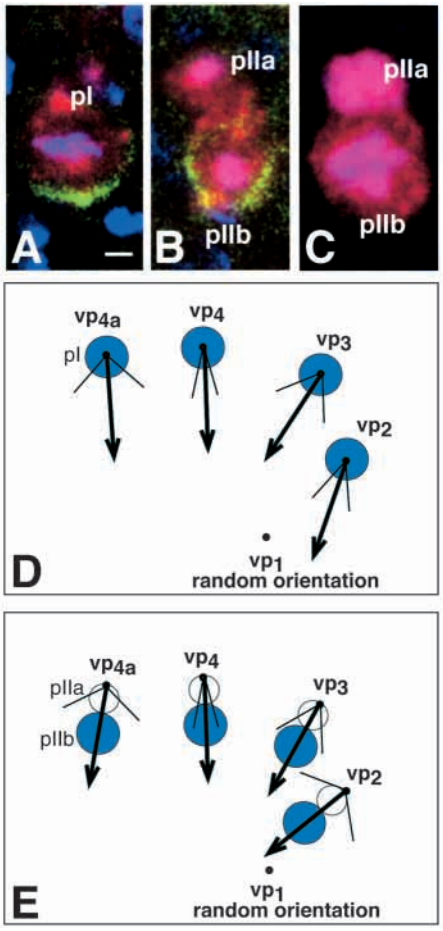

Fig. 3. The vp2-vp4a pI cells divide with a stereotyped dorsal-ventral planar polarity. (A-C) The polarity of the pI division was examined in stage 11-12 embryos stained for Cut (in red), Numb (in green) and DNA (in blue). Numb localises asymmetrically to the ventral pole at metaphase in the vp4a pI cell (A) and is inherited by the ventral pI daughter cell at telophase (B). The pIIa and pIIb nuclei remain within the plane of the epithelium. At stage 12, the ventral pI daughter cell, i.e. pIIb, enters mitosis (C). (D) The orientation of the planar division of pI was determined by measuring the angle between the d-v axis of the embryo and a vector that originates in the centre of pI and that points towards the centre of the Numb crescent. The angle value is between 0° and 180° when the Numb crescent is positioned anteriorly, and between 0° and –180° when the Numb crescent is positioned posteriorly. The mean value is indicated by an arrow and the standard deviation by a sector. The following orientations were measured: vp2, 19°±23 (*n*=30); vp3, 33°±35 (*n*=19); vp4, –2°±14 (*n*=30); vp4a, –4°±45 (*n*=30). (E) The position of the secondary precursor cell that divides first was determined as described above by measuring the angle between the d-v axis and a vector that joins the two pI daughter nuclei and points towards the dividing cell. The mean value is indicated by an arrow and the standard deviation by a sector. The following orientations were measured: vp2, 51°±60 (*n*=30); vp3, 29°±31 (*n*=30); vp4, –2°±13 (*n*=30); vp4a, 10°±54 (*n*=30). The cells that divide are in blue in D,E. In this and following Figs, unless noted otherwise, anterior (A) is towards the left and dorsal (D) is upwards. Scale bar: 3.5 μm.

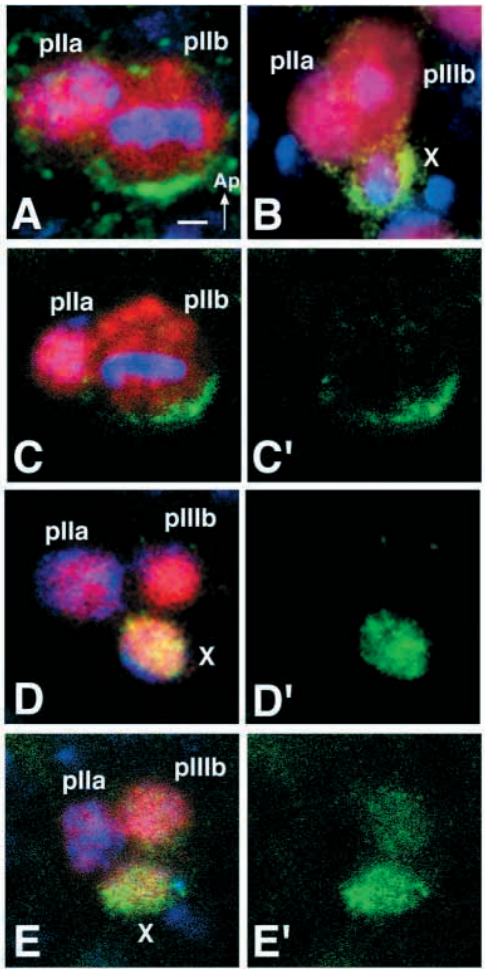

Fig. 4. pIIb divides asymmetrically with an apical-basal polarity. Sensory organ cells at the vp4 (A,B) and vp4a (C-E′) positions were labelled with Cut (in red), and dividing cells were identified by DNA staining (in blue). Numb (A,B) and Pros (C-E′) are in green. Apical (Ap) is upwards. Numb and Pros localise asymmetrically to the basal pole of pIIb at metaphase (A,C,C′) and segregate to the basal pIIb daughter cell at telophase (B,D,D′). At telophase, a difference in the size of the pIIb daughter cells is observed, with the basal cell being significantly smaller than its apical sister (B). Following this division, two Pros-positive cell are observed: a highly Pros-positive basal X cell and a weakly Pros-positive apical pIIIb cell (E-E′). Scale bar: 3.5 μm.

circular arc, while the vp4a X cell migrates dorsally. Consistent with a migratory behaviour, the X cells display long cytoplasmic extensions at this stage (Fig. 5E). The level of Pros accumulation in the migrating Cut- and Elav-positive X cells appears to decrease over time, and becomes undetectable when these cells cluster in the centre of the circular arc at stage 14. At this stage, these Cut-positive X cells can still be identified on the basis of their stereotyped position and of their high level of Elav accumulation. These cells occupy the positions of the $vda_{A\text{-}D}$/vbp cluster and of the vdaa neurone and, from stage 14 onwards, express the E7-2-36 md marker (Fig. 6C-C‴, Bier et al., 1989). These data indicate that the vp4a X cell migrates dorsally and becomes the vdaa md neurone, whereas the four vp1-vp4 X cells migrate towards the centre of the circular arc to form four of the five $vda_{A\text{-}D}$/vbp neurones. The fifth $vda_{A\text{-}D}$/vbp neurone corresponds to the additional Cut-, Pros- and Elav-positive cell that migrates (together with the vp1 md neurone) towards the centre of the circular arc (Fig. 6A-A‴).

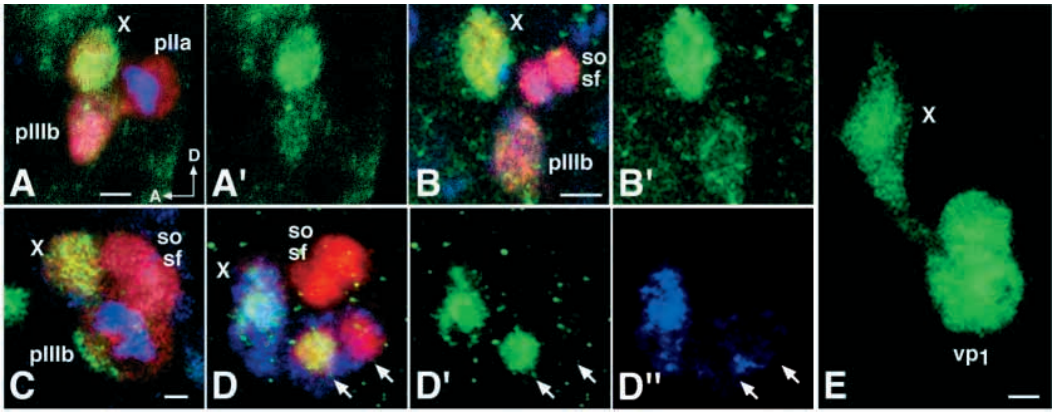

Fig. 5. pIIa and pIIIb cells divide, producing a total of five cells. (A-D″) Sensory organ cells at the vp2 position were identified by anti-Cut staining (in red). Pros is in green (A-D′), and Elav is in blue (D-D″). Mitoses were identified by DNA staining (in blue in A-C). (A,A′) The Pros-negative pIIa cell enters mitosis. Numb is asymmetrically localised in dividing pIIa and is inherited by one of the two daughter cells (data not shown). The X cell is subepidermal, but appears next to the pIIa and pIIIb cells, owing to the projection of several confocal *z* sections. (B-B′) Four cells are observed: the subepidermal X cell, the pIIIb cell and two highly Cut-positive, Pros-negative cells that are identified as the socket (so) and shaft (sh) cells. (C-D″) The pIIIb cell, identified as the weakly Pros-positive cell in B and B′, divides next (C, metaphase; D-D″, telophase). Elav accumulates at a high level in the X cell and at a low level in the dividing pIIIb (D-D″). Pros is asymmetrically localised at metaphase (C) and is inherited by only one daughter cell at telophase (arrows in D′), whereas Elav segregates to both daughter cells (arrows in D″). (E) At stage 13, the X cell of the vp1 organ, identified according to its position, displays long cytoplasmic extensions as revealed by β-galactosidase staining (green) in CutA3 embryos. Scale bars: in A, 7 μm for A,A′; in B, 7 μm for B,B′; in C, 3.5 μm for C-D″; in E, 7 μm for E.

This fifth md neurone probably originates from a Cut-positive precursor cell detected anterior to vp1. This precursor cell divides asymmetrically at late stage 12 to generate a Pros- and Elav-positive cell that migrates dorsally (see brackets in Fig. 2B-C′).

The es neurone and sheath cell are born from the pIIIb cell

From stage 14 onwards, one of the two pIIIb daughter cells accumulates a higher level of Elav, and is therefore identified as the es neurone (Fig. 6B″). Its sister cell accumulates a high level of Pros and is thus identified as the sheath cell (Fig. 6B′). No additional division is observed in the vp1-vp4a lineages after the pIIIb division.

In summary, this analysis shows that the vp1-vp4 es SOPs do not follow a solo-es lineage, as previously proposed, but rather produce four md neurones that most likely correspond to the four $vda_{A\text{-}D}$ organs (see Discussion). The vp4a SOP follows an identical lineage and generates the vdaa md neurone. In this novel md-es lineage, the md neurone is generated by the division of the pIIb cell.

insc is specifically expressed in the pIIb cell

Our detailed analysis of the vp1-vp4a lineages allowed us to investigate the mechanisms regulating cell polarity in these lineages. In this paper, we analyse the role of the *insc* gene. Previous studies have indicated that *insc* is expressed in pI, suggesting a role for *insc* in regulating cell polarity in these lineages (Knirr et al., 1997; Kraut and Campos-Ortega, 1996). However, previous studies of *insc* mutant embryos have failed to reveal a role of *insc* in the es lineages (Knirr et al., 1997; Kraut et al., 1996; Schober et al., 1999). In a first step, we have re-examined the expression pattern of *insc* in the vp1-vp4a lineages. We found that the Insc protein is not detectable in dividing pI, pIIa and pIIIb cells, but specifically accumulates in an apical crescent in dividing pIIb cells (Fig. 7A-C′ and data not shown). The lack of *insc* expression in pI is further confirmed by the analysis of an *insc-lacZ* enhancer-trap marker that has been previously used to document the expression of *insc* in pI cells in single-labelling experiments (Kraut and Campos-Ortega, 1996). The expression of *insc-lacZ* is not detectable in pI and pIIa. However, it is first detected in the pIIb cell as it divides and specifically accumulates in both pIIb daughter cells (Fig. 7D-F′).

insc regulates the apical-basal polarity of the pIIb division

We next analysed the role of *insc* in regulating cell polarity in the vp1-vp4a lineages. In *insc* mutant embryos, the vp1-vp4a pI divisions occur within the plane of the epithelium. The vp2, vp4 and vp4a pI cells divide with a d-v orientation with Numb localising asymmetrically to the ventral pole of pI (Fig. 8A). Furthermore, the cell that divides next is always found at an antero-ventral position in both wild-type and *insc* mutant embryos (compare Fig. 3E with Fig. 8B), suggesting that the pIIa and pIIb cells are correctly specified. We conclude that the loss of *insc* activity does not affect the polarity of the pI division. This is entirely consistent with our observation that the Insc protein is not present in the pI cell.

To analyse the role of *insc* in the dividing pIIb cell, we studied the asymmetric distribution of Miranda, an adaptor protein for Pros (Ikeshima-Kataoka et al., 1997; Shen et al., 1997). In wild-type embryos, Miranda accumulates to the basal pole of pIIb at metaphase (Fig. 8C,C′,H). In contrast, Miranda localises asymmetrically to the basal pole in only 32% of *insc* mutant pIIb cells at metaphase. In the other pIIb cells, Miranda is either partly (52%) or largely (16%) delocalised around the cell cortex (Fig. 8D-E′,H). This shows that *insc* is required for the basal localisation of Miranda.

We then analysed the distribution of Pros, which is the earliest marker for the fate of the md and pIIIb cells in the vp1-vp4a lineages (Figs 4E,E′, 8F,F′). We found an equal level of

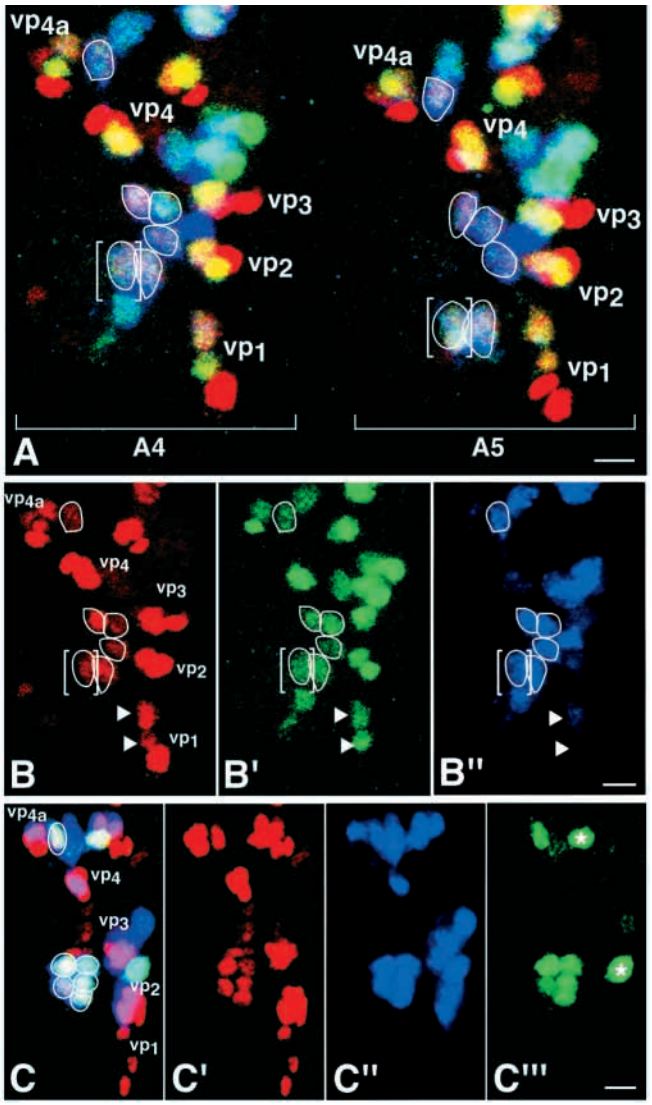

Fig. 6. The migrating X cell becomes an md neurone. (A-B″) Sensory organ cells at the vp1-vp4a positions were analysed in embryos stained for Cut (in red), Pros (in green) and Elav (in blue). At late stage 13, the positions of the four X cells produced by the vp1-vp4 lineages vary from one segment to the next (compare segments A4 and A5 in panel A), suggesting that these cells migrate towards the position of the vda_{A-D}/vbp cluster. One additional Cut-, Pros- and Elav-positive cell is seen just anterior to the vp1 X cell (brackets in A-B″). (B-B″) Separate channels are displayed for the segment A4 shown in A. The five X cells (outlined) accumulate Cut (B), Pros (B′) and Elav (B″). The two pIIIb daughter cells are Pros-positive, whereas Elav starts to accumulate in only one pIIIb daughter cell (see arrowheads at the vp1 position in B-B″). At later stages, the level of Pros accumulation decreases in the Elav-positive cell and concomitantly increases in the Elav-negative cell (not shown). (C-C‴) md neurones were identified in late stage 14 embryos stained for Cut (in red), Elav (in blue) and E7-2-36 (in green). The vp4a X cell is shown to express the E7-2-36 md marker, identifying it as the vdaa neurone. The four vp1-vp4 X cells also express this md marker and are found at the position of the vda_{A-D}/vbp cluster (outlined in C). The fifth cell of the vda_{A-D}/vbp cluster is probably the cell that migrates together with the vp1 X cell (brackets in A-B″). Asterisks in C‴ indicate the vdap and v'dap md neurones. Scale bars: in A, 5 μm; in B, 5 μm for B-B″; in C, 5 μm for C-C‴.

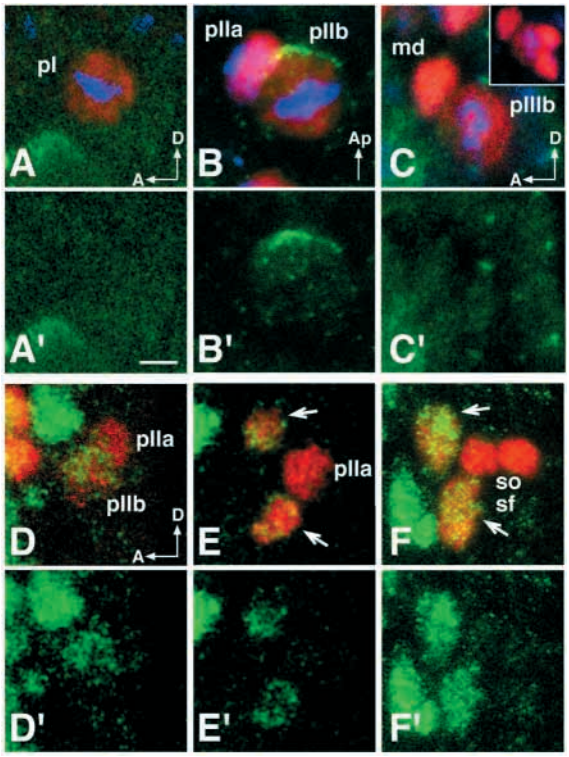

Fig. 7. Insc is specifically localised at the apical pole of the dividing pIIb cell. (A-C′) The accumulation of Insc (in green) was analysed in embryos stained for Cut (in red) and the DNA (in blue). Insc is not detected in dividing pI (A,A′) and pIIIb (C,C′) cells, and is detected at the apical pole of dividing pIIb cells (B,B′). The confocal *z* sections showing the subepidermal pIIIb and md cells were projected in C,C′. The socket and shaft cells that lie in the epidermis can be seen in the inset shown in C, for which the whole stack was projected. (A,A′,C,C′). Anterior is towards the left and dorsal is upwards. (B,B′) Apical is upwards. In A,A′,C,C′, the green channel was set at a higher gain than in B, B′ to show the absence of Insc accumulation in pI and pIIIb. (D-F′) The expression of *insc-lacZ* was studied in embryos heterozygous for the AB44 enhancer-trap insertion and stained for Cut (in red) and β-galactosidase (in green). The β-galactosidase protein is first detected in dividing pIIb cells (D,D′; the diffuse Cut staining in D identifies the pIIb cell as it divides). The β-galactosidase protein is seen to accumulate equally in both pIIb daughter cells (arrows in E). Following the division of the precursor giving rise to the socket and shaft cells, the β-galactosidase protein is absent from the socket and shaft cells (F,F′) and accumulates in the two other Cut-positive cells (arrows in F). Because of its stability and of its equal distribution at mitosis, the β-galactosidase protein could be used as a marker for the pIIb daughter cells. At stage 13, the β-galactosidase is not detected in the socket and shaft cells, implying that these two cells are not born from a pIIb daughter cell. The socket and shaft cells are therefore generated by the division of the pIIa cell (Fig. 7F-F′). Since we have shown that the socket and shaft cells are generated by a Pros-negative precursor cell (Figs 2C, 5A-B′), we conclude that this Pros-negative precursor cell is pIIa and that the two Pros-positive md and pIIIb cells are pIIb daughter cells. This analysis of the expression of *insc-lacZ* demonstrates that the weakly Pros-positive cell, that we called pIIIb (Fig. 4E,E′), is a pIIb daughter cell. Scale bar: 7 μm.

Pros accumulation in 27% of the pIIb daughter cells in *insc* mutant embryos (Fig. 8G,G′,I). This indicates that *insc* is required to regulate the unequal segregation of Pros during the

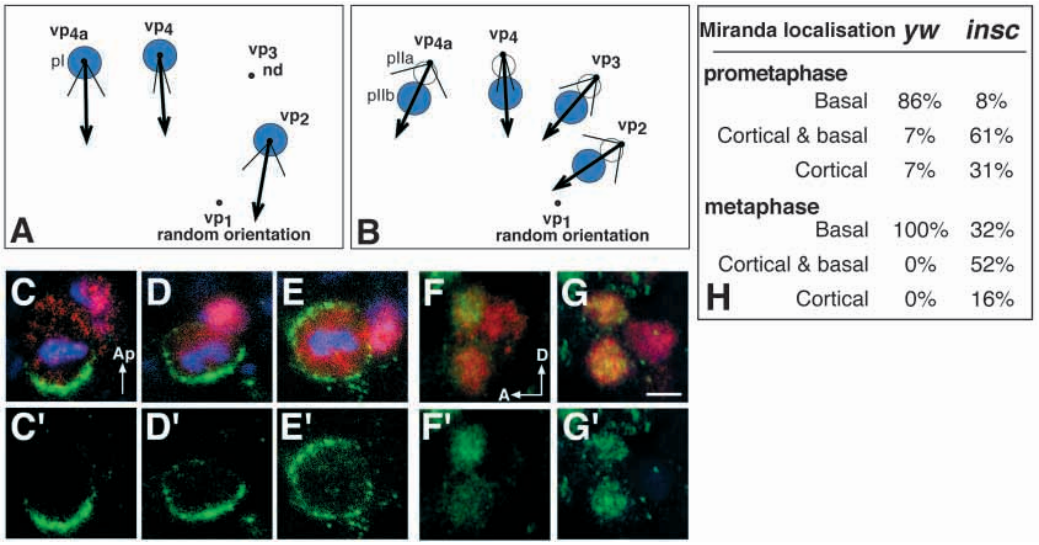

Miranda localisation	*yw*	*insc*
prometaphase		
Basal	86%	8%
Cortical & basal	7%	61%
Cortical	7%	31%
metaphase		
Basal	100%	32%
Cortical & basal	0%	52%
Cortical	0%	16%

H

Fig. 8. Insc regulates the apical-basal polarity of the pIIb cell division. (A,B) The orientation of the planar division of pI (A) and the position of the cell that divides next (B) were analysed in *insc* mutant embryos, as described in the legend to Fig. 3. The following orientations were measured: vp2, 10°±34 (*n*=30); vp4, –4°±12 (*n*=30); vp4a, –1°±28 (*n*=30) in A, and vp2, 56°±47 (*n*=30); vp3, 41°±32 (*n*=30); vp4, –3°±12 (*n*=30); vp4a, 25°±50 (*n*=30) in B. The loss of *insc* activity has no effect on the polarity and orientation of the pI division. nd, not determined. (C-E′) The distribution of Miranda (in green) in dividing pIIb cells was analysed in embryos stained for Cut (in red) and the DNA (in blue). In wild-type embryos, Miranda localises to the basal pole of pIIb at metaphase (C,C′). In *insc* mutant embryos, Miranda can be found either at the basal pole (not shown), partly delocalised from the basal pole (D,D′) or uniformly distributed at the cell cortex (E,E′) at metaphase. Apical is upwards and anterior is towards the left in C-E′. (F-G′) The accumulation of Pros (in green) in the pIIb daughter cells was studied in embryos stained also for Cut (in red). In wild-type embryos, the Pros staining is stronger in the basal pIIb daughter cell than in the apical pIIb daughter cell in 99% of the case (*n*=100) (F,F′). In contrast, Pros accumulates to similar levels in the two pIIb daughter cells in 27% of the cases (*n*=136) (G-G′). Anterior is towards the left and dorsal is upwards. Note that in this projection the basal pIIb daughter cell appears dorsal (F,F′). (H) Quantification of the Miranda localisation phenotype, at prometaphase in wild-type (*n*=14) and *insc* mutant (*n*=13) embryos and at metaphase in wild-type (*n*=20) and *insc* mutant (*n*=20) embryos. Scale bar: 3.5 μm.

pIIb division and/or to establish a fate difference between the two pIIb daughter cells.

insc regulates the fate of the md neurone and of the pIIIb cell

We then investigated the role of *insc* in regulating cell fate decisions in the vp1-vp4a lineages. We initially focused our attention on the vp4a organ because this lineage generates one md neurone that migrates very little, which greatly facilitates the identification of all the cells produced by the vp4a lineage. We used Cut, Elav and E7-2-36 as cell fate markers to identify the vp4a socket, shaft and sheath cells, and the es neurone and the vdaa md neurone at stage 16 (Fig. 9A). At all vp4a positions in *insc* mutant embryos, the socket and shaft cells are always present. In some segments, however, the vdaa md neurone is duplicated and the vp4a es neurone and sheath cell are missing (Fig. 9B). This suggests that the pIIIb cell has been transformed into a second md neurone. In some other segments, a single Elav-positive, E7-2-36-negative cell is seen at the position of the vp4a es neurone and sheath cell (Fig. 9C). This suggests that the pIIIb cell has failed to divide. In yet other segments, the two cells at the position of the es neurone and sheath cell express variable levels of Elav, indicating that the two pIIIb daughter cells are not correctly specified (Fig. 9D). We conclude that *insc* regulates the fate of the pIIb daughter cells.

We next extended this analysis to the vp1-vp4 lineages (Fig. 9E-H). As shown for the vp4a organ, the socket and shaft cells are always detected, while the neurone and sheath cells form properly in only 66% (*n*=124) of the vp1-vp4 organs. In 22% of the cases, the two cells at the position of the sheath cell and es neurone express a similar level of either Elav (see vp2 in Fig. 9H), or Pros (see vp1 in Fig. 9H), or both Pros and Elav (not shown). In 6% of the es organs, only one Elav-expressing cell is detected. Finally, in the remaining 6%, the es neurone and sheath cell are both missing. This defect is always associated with the presence of an additional md neurone at the $vda_{A\text{-}D}$/vbp position (7 cases out of 7, see vp4 in segment A6 in Fig. 9G and vp1 in Fig. 9F). This indicates that the pIIIb cell has been transformed into an md neurone.

In some segments (*n*=3/31), the presence of one additional md neurone at the $vda_{A\text{-}D}$/vbp position could not be correlated with a defect in the number of the vp1-vp4 organ cells (see segment A5 in Fig. 9G). We interpret this phenotype as a cell fate transformation in the lineage of the Cut-positive precursor cell detected anteriorly to vp1, which would generate two md neurones in *insc* mutant embryos. Consistent with this hypothesis, *insc-lacZ* is expressed in this lineage (data not shown).

In conclusion, our data show that the loss of *insc* activity results in cell polarity defects in the pIIb cell, as revealed by the mislocalisation of Miranda at metaphase. This phenotype correlates with the abnormal accumulation of Pros into the apical pIIb daughter cell and with the mis-specification of the pIIIb cell.

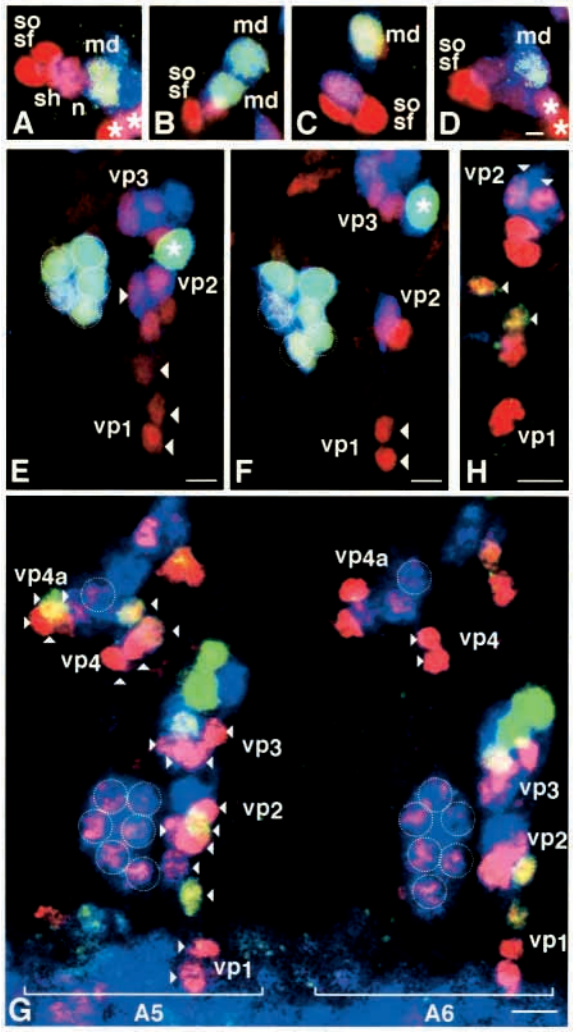

Fig. 9. Insc regulates the fates of the pIIb daughter cells. (A-F) Stage 16 wild-type (A,E) or *insc* mutant (B-D,F) embryos are stained for Cut (in red), Elav (in blue) and β-galactosidase (E7-2-36; in green). (A-D) At the vp4a position, a single vdaa neurone is seen together with the four vp4a cells in wild-type embryos (A), whereas various defects may be observed in *insc* mutant embryos (B-D): a loss of the vp4a es neurone and sheath cell accompanied by a duplication of the vdaa md neurone (B); a single Elav-positive cell seen at the position of the vp4a es neurone and sheath cell (C); or the presence of two pIIIb daughter cells accumulating Elav (D). In contrast, the socket and shaft cells were always correctly specified (B-D). Asterisks indicate vp4 organ cells. (E,F) In wild-type embryos (E), five vda_{A-D}/vbp neurones are detected, while in *insc* mutant embryos (F), one extra Cut-positive, Elav-positive and E7-2-36-positive cell can be observed at the position of vda_{A-D}/vbp neurones (outlined by broken circles in E and F). This phenotype is accompanied by the loss of the vp1 es neurone and sheath cell (compare arrowheads pointing to the vp1 organ cells in E and F, the vp1 neurone in E was identified based on its Elav-positive dendritic extension). The Cut-negative, ASC-independent vdap md neurones are indicated by asterisks. (G) Six Cut- and Elav-positive cells were seen at the position of vda_{A-D}/vbp neurones in the segments A5 and A6 of a *insc* mutant embryos stained for Cut (in red), Pros (in green) and Elav (in blue). Broken circles outline the vda_{A-D}/vbp and vdaa md neurones. In the segment A6, the neurone and the sheath cell of the vp4 organ are absent (arrowheads point toward the remaining socket and shaft cells) while all vp1 to vp4a es organ cells are present in the segment A5 (arrowheads point to every cell of the vp1 to vp4a organs). The phenotype observed in the segment A6 is similar to the phenotype described in F. In contrast, the correct number of vp1-vp4 es cells is seen in the segment A5. (H) In this *insc* mutant embryo stained for Cut (in red), Pros (in green) and Elav (in blue), the pIIIb daughter cells accumulate equal amount of either Elav (see vp2) or Pros (see vp1). Equal accumulation of Elav in both pIIIb daughter cells is also observed in the vp4a organ of the segment A6 in G. Scale bars: in D, 3.5 μm for A-D; in E-G, 5 μm.

DISCUSSION

A novel model for the mono-innervated md-es lineage

We have described the complete lineages generated by the five vp1-vp4a SOPs. Prior to this study, the vp1-vp4 lineages were considered to be of the solo-es type, while the vp4a lineage was described as an md-es lineage (Brewster and Bodmer, 1995). In contrast to this classification, our analysis reveals that the same lineage applies to the five ventral papilla. We confirm that the vp4a lineage produces the vdaa md neurone and we propose that the vp1-vp4 lineages generate four of the five vda_{A-D}/vbp neurones. The four md neurones produced by the vp1-vp4 SOPs are likely to be the vda_{A-D} neurones since embryos carrying deletions for the *Achaete-scute Complex* (*ASC*) lack all four vp1-vp4 es organs together with the four vda_{A-D} md neurones, while the vbp neurone remains unaffected (Dambly-Chaudière and Ghysen 1986). This indicates that the vbp neurone is produced by an unrelated lineage. Our data suggest that the vbp neurone is produced by the asymmetric division of a precursor cell found anteriorly to the vp1 cells.

We propose a novel model for the mono-innervated es-md lineage, in which each pI cell undergoes a series of four asymmetric divisions to generate the four es cells and one md neurone (Fig. 10A). This model differs from the three models previously proposed for the es lineages (Fig. 10D-F). Based on BrdU incorporation, Bodmer et al. have shown that the socket and shaft cells are born from a precursor cell that replicates its DNA prior to the precursor cell that generates the neurone and the sheath cell (Bodmer et al., 1989). These observations are consistent with the lineage proposed here. However, assuming that the SOP cell generates only the four cells of the mature es organs, Bodmer et al. proposed a model where each SOP cell generates two secondary precursor pIIa and pIIb which divide once to produce the four es organ cells (Fig. 10D). In a more recent study based on the retrospective analysis of small *lacZ*-positive FLP-out clones, Brewster and Bodmer proposed that the vp1-vp4 SOPs follow a solo-es lineage (Fig. 10D), while the vp4a SOP produces the vp4a es organ together with the vdaa md neurone (Fig. 10E; Brewster and Bodmer, 1995). This lineage differs from the solo-es lineage by the existence of an additional round of asymmetric division that produces the es neurone and the md neurone. As mentioned by the authors, this analysis did not allow to definitively conclude that the vdaa and vp4a neurones are sister cells (Brewster and Bodmer, 1995). In fact, BrdU-labelling experiments indicate that the precursor of the vdaa neurone replicates its DNA prior to the precursor cells that generate the four vp4a cells (Bodmer et al., 1989). This

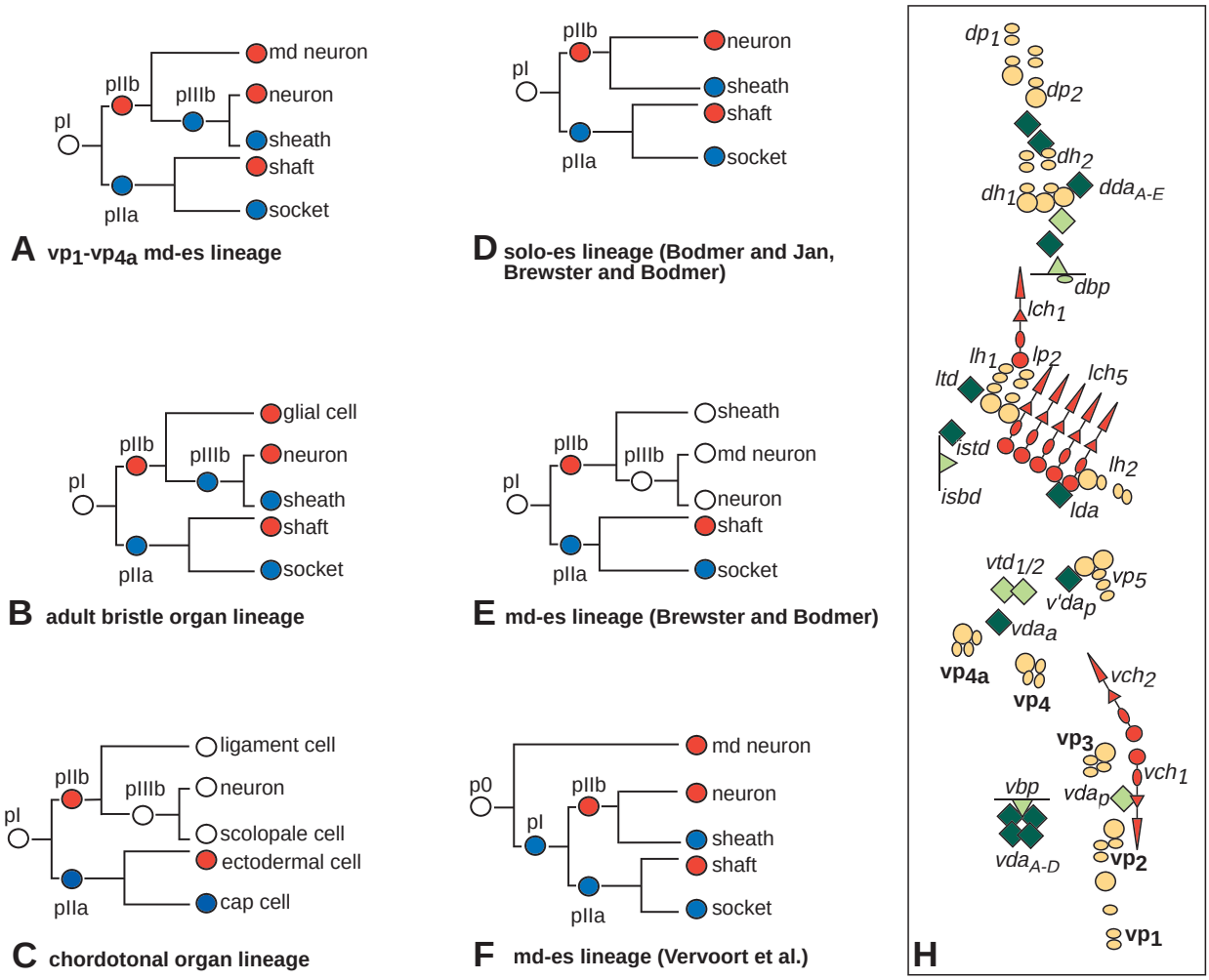

Fig. 10. A novel model for the md-es lineage. (A-H) The different models that have been proposed for the sensory organ lineages in *Drosophila*. The daughter cells that specifically inherit Numb at mitosis are in red. The cells in which Notch signalling is (presumably) activated are in blue. The md-es lineage proposed here for the vda_{A-D}/vp1-vp4 and vdaa/vp4a organs is shown in A. This lineage is similar to the ones proposed for the adult mechanosensory bristles (Gho et al., 1999) (B) and for the larval chordotonal organs (Brewster and Bodmer, 1995) (C). In the chordotonal organ lineage, Numb segregation was deduced from the interpretation of the *numb* mutant phenotype (Uemura et al., 1989). In the mechanosensory organs of the wing margin, the glial cell can undergo at least one round of symmetrical division to generate additional glial cells (Van De Bor et al., 2000). (D) The model initially proposed for all the mono-innervated es lineage (Bodmer et al., 1989) and subsequently for the solo-es lineage generating in particular the vp1-vp4 organs (Brewster and Bodmer, 1995). (E) The model proposed for the md-es lineage, that generates the vp4a organ together with the vdaa neurone (Brewster and Bodmer, 1995). (F) The model proposed by Vervoort et al. for the md-es lineage (Vervoort et al., 1997). (H) The PNS in the abdominal segments A1-7 (adapted, with permission, from Brewster and Bodmer, 1995). The es and chordotonal organs are shown in yellow and red, respectively, while md neurones are shown in green. The number of ASC-dependent md neurones (dark green) exactly matches the number of es organs. The md neurones that remain in *AS-C* mutant embryos are in light green. These neurones are therefore thought to be produced by lineages unrelated to the es organ lineage (Dambly-Chaudière and Ghysen, 1986).

observation is consistent with the lineage proposed here, but excludes the lineage proposed by Brewster and Bodmer (Brewster and Bodmer, 1995).

More recently, Vervoort et al. revised the md-es lineage and proposed the existence of a p0 cell that would divide asymmetrically to give rise to an es pI cell and to an md neurone (Fig. 10F; Vervoort et al., 1997). This hypothesis was based on the lack of md neurones and on the excess of external accessory es cells in *numb* mutant embryos, and, conversely, on the excess of md neurones and lack of es neurones in *Notch* mutant embryos. These observations led Vervoort et al. to propose that the cell that inherits Numb during the postulated p0 division is the md neurone (Vervoort et al., 1997). This hypothesis is, however, not consistent with our observation that the cell receiving Numb during the first division undergoes two additional rounds of cell division. As discussed below, the model proposed here can also account for these *numb* and *Notch* mutant phenotypes. Thus, together with the BrdU-labelling data presented by Bodmer et al. (Bodmer et al., 1989), our study of the vp1-vp4a lineages rules out all three previously proposed models for the md-es lineage.

The pattern of cell divisions is identical in the vp1-vp4a, chordotonal and adult bristle lineages

We and others have recently proposed a novel model for the lineage of the adult mechanosensory organs in the notum (Fig. 10B; Gho et al., 1999; Reddy and Rodrigues, 1999). The direct observation of cell divisions by time-lapse microscopy has shown that each pI cell undergoes a series of four asymmetric cell divisions to generate the four cells composing one es organ as well as one glial cell (Gho et al., 1999). This lineage is strikingly similar to the one proposed here for the vp1-vp4a organs.

Moreover, the md-es lineage proposed here is also similar to the chordotonal lineage proposed by Brewster and Bodmer (Brewster and Bodmer, 1995; Fig. 10C). In this lineage, the pIIb cell divides to generate a ligament cell and a pIIIb cell, which in turn divides to generate a neurone and a scolopale cell, while the pIIa cell divides asymmetrically to produce the cap cell and an ectodermal cell.

Based on these lineage relationships, we propose that the md neurone in the md-es lineage is the homolog of the glial and ligament cells in the bristle and chordotonal lineages, respectively. Interestingly, both the glial cell in the pupa and the ligament cell in the embryo express *repo* and *glial cells missing* (*gcm*) (Gho et al., 1999; Halter et al., 1995; Hosoya et al., 1995; Jones et al., 1995; Reddy and Rodrigues, 1999; Van De Bor et al., 2000). Furthermore, both cells adopt a neuronal fate in *gcm* mutant conditions (Hosoya et al., 1995; Jones et al., 1995; Van De Bor et al., 2000; Y. B., unpublished observations). Whether this transformed neurone shows the large dendritic arborisation typical of md neurones remains to be examined. We propose that each SOP follows an invariant sequence of asymmetric cell divisions, and that variations in the fate of the progeny cells depends on the combinatorial expression of proneural and selector genes, such as *cut* or *gcm*.

Should the other solo-es and md-es lineages be also revised?

Since the results from previous lineage studies were interpreted with the assumption that little or no cell migration occurs during PNS development, an md-es lineage could only be recognised when a ASC-dependent md neurone is located close to a es organ. Thus, four md-es pairs were established: vp4a and vdaa; lh2 and lda; lp2 and ltd; and dh1 and one of the five dda_{A-E} md neurones. Similarly, an md-poly-innervated-es lineage was proposed for the following two pairs: vp5 and v'dap; dh2 and one of the five ddaA-E md neurones (Brewster and Bodmer, 1995). Here, we have established four new md-es pairs: vp1-vp4 and the four vda_{A-D} md neurones. We propose that the remaining three ASC-dependent md neurones, istd and two of the three dda_{A-E} neurones (Dambly-Chaudière and Ghysen, 1986), are also related by lineage to the lh1, dp1 and dp2 organs, respectively. Thus, each es organ can be associated with a ASC-dependent md neurone. We therefore propose that the lineage described here for the vp1-vp4a lineages applies to all mono-innervated es organs in the embryo.

Implications for the interpretation of mutant phenotypes

Consistent with a unique md-es lineage, mutations affecting the Notch signalling pathway lead to similar transformations in all mono-innervated es organs. Based on our description of the asymmetric segregation of Numb to the pIIb cell and to the md neurone during the formation of the vp1-vp4 organs (Fig. 10A), we propose a novel interpretation of the mutant phenotypes in genes involved in the Notch pathway. *Notch* mutant embryos have a large excess of md neurones and a loss of es neurones and es accessory cells (Vervoort et al., 1997), which we interpret as a pIIa-to-pIIb transformation followed by a pIIIb-to-md neurone transformation. Similarly, *sanpodo* mutant embryos display an excess of md neurones and a loss of sheath cells, which we interpret as a pIIIb-to-md neurone transformation (Dye et al., 1998; Salzberg et al., 1994; Salzberg et al., 1997). Finally, *numb* mutant embryos show a complete loss of md neurones, es neurones and sheath cells, together with a doubling in the number of socket and shaft cells (Uemura et al., 1989; Vervoort et al., 1997). This phenotype can be interpreted as a pIIb-to-pIIa transformation.

The function of Insc in the md-es lineage

We have found that Insc does not accumulate in the pI cell but forms an apical crescent only in the pIIb cell. This contrasts with previous studies suggesting that the *insc* gene is expressed in pI (Knirr et al., 1997; Kraut and Campos-Ortega, 1996). These studies, however, did not rely on double labelling experiments to identify the pI cell. Therefore, it is possible that pIIb cells might have been mistaken for pI cells. Consistent with this observation, we found that the polarity of the pI cell division does not depend on the activity of the *insc* gene (see also Schober et al., 1999). In contrast, the asymmetric division of pIIb, which is polarised along the apical-basal axis, depends on the *insc* activity. During the division of pIIb, Pros, Miranda, Numb and Pon specifically segregate to the basal md neurone. Using Miranda as a marker for cell polarity, we have shown that the *insc* activity is required to polarise the pIIb cell along its apical-basal axis. As also seen in neuroblasts (Yu et al., 2000), the complete zygotic loss of *insc* function results only in a partial delocalisation of the basal Miranda crescent in the pIIb cell. Consistent with this defect in cell polarity, the unequal accumulation of Prospero in the two pIIb daughter cells is affected, and the fates of the pIIb daughter cells are not correctly specified. Indeed, the loss of *insc* activity can result in the pIIIb cell adopting an md fate. It can also lead to the abnormal differentiation of the pIIIb daughter cells. As Insc does not form a crescent in the pIIIb cell, this latter phenotype is probably an indirect consequence of the mis-specification of the pIIIb cell fate following the pIIb division.

Insc is known to regulate both cell polarity and cell fate decisions in several asymmetrically dividing cells in the mesoderm and in the CNS. In the dividing GMC 4.2, Numb segregates to the RP2 neurone and is required for the specification of the RP2 fate. In *insc* mutant embryos, a second RP2 neurone forms at the expense of the RP2 sib neurone, indicating that the loss of *insc* activity promotes the fate adopted by the cell inheriting Numb in wild-type embryos (Buescher et al., 1998). Similarly, in *insc* mutant embryos, we observed some pIIIb-to-md transformations but never the reciprocal md-to-pIIIb transformation, indicating that the loss of *insc* function promotes the fate of the cell receiving Numb.

Cell polarity and asymmetric divisions in the embryonic PNS

This study provides the first detailed description of each

asymmetric cell division in an md-es lineage. The division of the vp2-vp4a pI cell is planar and takes place with a d-v polarity, revealing for the first time the existence of a planar polarity orienting asymmetric cell divisions in the embryo. Similarly, in the pupa, the pI cell divides in the plane of the epithelium and along the a-p axis (Gho et al., 1999; Gho and Schweisguth, 1998). The polarity of this division is controlled by the Fz signalling pathway (Gho and Schweisguth, 1998). Future studies will address whether the polarity of the pI cell division of vp2-vp4a organs is controlled by similar mechanisms.

In both pupae and embryos, the pIIb cell divides with an apical-basal polarity, with Numb, Pros and Miranda segregating to the basal cell (Gho et al., 1999; V. O., F. S. and Y. B., unpublished observations). Moreover, Insc forms an apical crescent in the pIIb cell in the pupal lineage (Y. B., unpublished observation). This suggests that Insc regulates also the apical-basal polarity of the pIIb cell in the adult bristle lineage. It is clear, however, that a detailed analysis of the function of *insc* in regulating cell polarity in the adult PNS would have been much more difficult and time-consuming because *insc* mutations are embryonic lethal.

In conclusions, this study clearly illustrates that the regulation of both planar and apical-basal polarities can now be studied in the embryonic PNS. This detailed analysis therefore provides the basis for future studies addressing the function of various candidate genes known to affect the development of the embryonic PNS.

We thank B Chia, C. Gonzalez, R. Jack, Y.-N. Jan, J. Knoblich, F. Matsuzaki and the DSHB for providing various antibodies and flies. We wish to thank the Imaging facility of the Institut Jacques Monod and Gérard Géraud for use of their confocal microscope. We also thank M. Gho and R. LeBorgne for critical reading of this manuscript. This work was supported by grants to F. S. from the Centre National de la Recherche Scientifique and Association pour la Recherche sur le Cancer (ARC 5575). V. O. was supported by the Ecole Normale Supérieure, and Y. B. was supported in part by an ARC post-doctoral fellowship.

Note added in proof

Consistent with the analogy between the pupal and embryonic es lineages documented here, Roegiers et al. have shown that the Inse protein accumulates in the pIIb cell of the adult bristle lineage, and regulates the orientation of the pIIb division in the pupa (Roegiers et al., 2001).

REFERENCES

Bellaïche, Y., Gho, M., Kaltschmidt, J. A., Brand, A. H. and Schweisguth, F. (2001). Frizzled regulates the localisation of cell-fate determinants and mitotic spindle rotation during asymmetric cell division. *Nat. Cell Biol.* **3**, 50-57.

Bier, E., Ackerman, L., Barbel, S., Jan, L. and Jan, Y. N. (1988). Identification and characterization of a neuron-specific nuclear antigen in Drosophila. *Science* **240**, 913-916.

Bier, E., Vaessin, H., Shepherd, S., Lee, K., McCall, K., Barbel, S., Ackerman, L., Carretto, R., Uemura, T., Grell, E. et al. (1989). Searching for pattern and mutation in the *Drosophila* genome with a P-lacZ vector. *Genes Dev.* **3**, 1273-1287.

Blochlinger, K., Bodmer, R., Jack, J., Jan, L. Y. and Jan, Y. N. (1988). Primary structure and expression of a product from *cut*, a locus involved in specifying sensory organ identity in *Drosophila*. *Nature* **333**, 629-635.

Blochlinger, K., Bodmer, R., Jan, L. Y. and Jan, Y. N. (1990). Patterns of expression of *cut*, a protein required for external sensory organ development in wild-type and *cut* mutant *Drosophila* embryos. *Genes Dev.* **4**, 1322-1331.

Bodmer, R., Carretto, R. and Jan, Y. N. (1989). Neurogenesis of the peripheral nervous system in *Drosophila* embryos: DNA replication patterns and cell lineages. *Neuron* **3**, 21-32.

Brewster, R. and Bodmer, R. (1995). Origin and specification of type II sensory neurons in *Drosophila*. *Development* **121**, 2923-2936.

Buescher, M., Yeo, S. L., Udolph, G., Zavortink, M., Yang, X., Tear, G. and Chia, W. (1998). Binary sibling neuronal cell fate decisions in the *Drosophila* embryonic central nervous system are nonstochastic and require *inscuteable*-mediated asymmetry of ganglion mother cells. *Genes Dev.* **12**, 1858-1870.

Campos-Ortega, J. A. and Hartenstein, V. (1997). Peripheral nervous system. In *The Embryonic Development of* Drosophila melanogaster, pp. 177-209. Berlin: Springer-Verlag.

Dambly-Chaudière, C. and Ghysen, A. (1986). Independent subpatterns of sense organs require independent genes of the *achaete-scute* complex in *Drosophila* larvae. *Genes Dev* **1**, 297-306.

Dye, C. A., Lee, J. K., Atkinson, R. C., Brewster, R., Han, P. L. and Bellen, H. J. (1998). The *Drosophila sanpodo* gene controls sibling cell fate and encodes a tropomodulin homolog, an actin/tropomyosin-associated protein. *Development* **125**, 1845-1856.

Gho, M. and Schweisguth, F. (1998). Frizzled signalling controls orientation of asymmetric sense organ precursor cell divisions in *Drosophila*. *Nature* **393**, 178-181.

Gho, M., Bellaiche, Y. and Schweisguth, F. (1999). Revisiting the *Drosophila* microchaete lineage: a novel intrinsically asymmetric cell division generates a glial cell. *Development* **126**, 3573-3584.

Grzeschik, N., Breuer, S., Renkawitz-Pohl, R. and Paululat, A. (1999). Molecular characterization of a point mutation in the *Drosophila inscuteable* gene. Drosophila *Information Service* 82, 27-29.

Halter, D. A., Urban, J., Rickert, C., Ner, S. S., Ito, K., Travers, A. A. and Technau, G. M. (1995). The homeobox gene *repo* is required for the differentiation and maintenance of glia function in the embryonic nervous system of *Drosophila melanogaster*. *Development* **121**, 317-332.

Hartenstein, V. and Posakony, J. W. (1989). Development of adult sensilla on the wing and notum of *Drosophila melanogaster*. *Development* **107**, 389-405.

Hirata, J., Nakagoshi, H., Nabeshima, Y. and Matsuzaki, F. (1995). Asymmetric segregation of the homeodomain protein Prospero during *Drosophila* development. *Nature* **377**, 627-630.

Hosoya, T., Takizawa, K., Nitta, K. and Hotta, Y. (1995). *glial cells missing*: a binary switch between neuronal and glial determination in *Drosophila*. *Cell* **82**, 1025-1036.

Ikeshima-Kataoka, H., Skeath, J. B., Nabeshima, Y., Doe, C. Q. and Matsuzaki, F. (1997). Miranda directs Prospero to a daughter cell during *Drosophila* asymmetric divisions. *Nature* **390**, 625-629.

Jack, J. and DeLotto, Y. (1995). Structure and regulation of a complex locus: the *cut* gene of *Drosophila*. *Genetics* **139**, 1689-1700.

Jan, Y. N., Bodmer, R., Jan, L. Y., Ghysen, A. and Dambly-Chaudiere, C. (1987). Mutations affecting the embryonic development of the peripheral nervous system in *Drosophila*. In *Molecular Entomology*, pp. 45-56. Proceedings of a Monsanto UCLA Symposium, Steamboat Springs, Colorado, USA

Jan, Y. N. and Jan, L. Y. (2000). Polarity in cell division: what frames thy fearful asymmetry? *Cell* **100**, 599-602.

Jones, B. W., Fetter, R. D., Tear, G. and Goodman, C. S. (1995). *glial cells missing*: a genetic switch that controls glial versus neuronal fate. *Cell* **82**, 1013-1023.

Kaltschmidt, J. A., Davidson, C. M., Brown, N. H. and Brand, A. H. (2000). Rotation and asymmetry of the mitotic spindle direct asymmetric cell division in the developing central nervous system. *Nat. Cell Biol.* **2**, 7-12.

Kania, A., Salzberg, A., Bhat, M., D'Evelyn, D., He, Y., Kiss, I. and Bellen, H. J. (1995). P-element mutations affecting embryonic peripheral nervous system development in *Drosophila* melanogaster. *Genetics* **139**, 1663-1678.

Knirr, S., Breuer, S., Paululat, A. and Renkawitz-Pohl, R. (1997). Somatic mesoderm differentiation and the development of a subset of pericardial cells depend on the *not enough muscles* (*nem*) locus, which contains the *inscuteable* gene and the intron located gene, *skittles*. *Mech. Dev.* **67**, 69-81.

Knoblich, J. A., Jan, L. Y. and Jan, Y. N. (1995). Asymmetric segregation of Numb and Prospero during cell division. *Nature* **377**, 624-627.

Kraut, R. and Campos-Ortega, J. A. (1996). *inscuteable*, a neural precursor

gene of *Drosophila*, encodes a candidate for a cytoskeleton adaptor protein. *Dev. Biol.* **174**, 65-81.

Kraut, R., Chia, W., Jan, L. Y., Jan, Y. N. and Knoblich, J. A. (1996). Role of *inscuteable* in orienting asymmetric cell divisions in *Drosophila*. *Nature* **383**, 50-55.

Lu, B., Rothenberg, M., Jan, L. Y. and Jan, Y. N. (1998). Partner of Numb colocalizes with Numb during mitosis and directs Numb asymmetric localization in *Drosophila* neural and muscle progenitors. *Cell* **95**, 225-235.

Parmentier, M.-L., Woods, D., Greig, S., Phan, P. G., Radovic, A., Bryant, P. and O'Kane, C. J. (2000). Rapsynoid/Partner of Inscuteable controls asymmetric division of larval neuroblasts in *Drosophila*. *J. Neurosci.* **20**, RC84, 1-5.

Reddy, G. V. and Rodrigues, V. (1999). A glial cell arises from an additional division within the mechanosensory lineage during development of the microchaete on the *Drosophila* notum. *Development* **126**, 4617-4622.

Rhyu, M. S., Jan, L. Y. and Jan, Y. N. (1994). Asymmetric distribution of numb protein during division of the sensory organ precursor cell confers distinct fates to daughter cells. *Cell* **76**, 477-491.

Roegiers, F., Younger Shepherd, S., Jan, L. Y. and Jan, Y. N. (2001). Two types of asymmetric divisions in the Drosophila sensory organ precursor cell lineage. *Nat. Cell Biol.* **3**, 58-67.

Salzberg, A., D'Evelyn, D., Schulze, K. L., Lee, J. K., Strumpf, D., Tsai, L. and Bellen, H. J. (1994). Mutations affecting the pattern of the PNS in *Drosophila* reveal novel aspects of neuronal development. *Neuron* **13**, 269-287.

Salzberg, A., Prokopenko, S. N., He, Y., Tsai, P., Pal, M., Maroy, P., Glover, D. M., Deak, P. and Bellen, H. J. (1997). P-element insertion alleles of essential genes on the third chromosome of *Drosophila melanogaster*: mutations affecting embryonic PNS development. *Genetics* **147**, 1723-1741.

Schaefer, M., Shevchenko, A. and Knoblich, J. A. (2000). A protein complex containing Inscuteable and the Galpha-binding protein Pins orients asymmetric cell divisions in *Drosophila*. *Curr. Biol.* **10**, 353-362.

Schober, M., Schaefer, M. and Knoblich, J. A. (1999). Bazooka recruits Inscuteable to orient asymmetric cell divisions in *Drosophila* neuroblasts. *Nature* **402**, 548-551.

Shen, C. P., Jan, L. Y. and Jan, Y. N. (1997). Miranda is required for the asymmetric localization of Prospero during mitosis in *Drosophila*. *Cell* **90**, 449-458.

Spana, E. P. and Doe, C. Q. (1995). The Prospero transcription factor is asymmetrically localized to the cell cortex during neuroblast mitosis in *Drosophila*. *Development* **121**, 3187-3195.

The, I., Bellaiche, Y. and Perrimon, N. (1999). Hedgehog movement is regulated through tout velu-dependent synthesis of a heparan sulfate proteoglycan. *Mol. Cell* **4**, 633-639.

Uemura, T., Shepherd, S., Ackerman, L., Jan, L. Y. and Jan, Y. N. (1989). *numb*, a gene required in determination of cell fate during sensory organ formation in *Drosophila* embryos. *Cell* **58**, 349-360.

Vaessin, H., Grell, E., Wolff, E., Bier, E., Jan, L. Y. and Jan, Y. N. (1991). *prospero* is expressed in neuronal precursors and encodes a nuclear protein that is involved in the control of axonal outgrowth in *Drosophila*. *Cell* **67**, 941-953.

Van De Bor, V., Walther, R. and Giangrande, A. (2000). Some fly sensory organs are gliogenic and require *glide*/*gcm* in a precursor that divides symmetrically and produces glial cells. *Development* **127**, 3735-3743.

Vervoort, M., Merritt, D. J., Ghysen, A. and Dambly-Chaudiere, C. (1997). Genetic basis of the formation and identity of type I and type II neurons in *Drosophila* embryos. *Development* **124**, 2819-2828.

Wodarz, A., Ramrath, A., Kuchinke, U. and Knust, E. (1999). Bazooka provides an apical cue for Inscuteable localization in *Drosophila* neuroblasts. *Nature* **402**, 544-547.

Yu, F., Morin, X., Cai, Y., Yang, X. and Chia, W. (2000). Analysis of *partner of inscuteable*, a novel player of Drosophila asymmetric divisions, reveals two distinct steps in Inscuteable apical localization. *Cell* **100**, 399-409.